

## Comparative Binding Analysis of N- Acetylneuraminic Acid in Bovine Serum Albumin and Human #-1 Acid Glycoprotein

Subramani Karthikeyan, Ganesan Bharanidharan, Sriram Raghavan, Saravanan Kandasamy, Shanmugavel Chinnathambi, Kanniyappan Udayakumar, Rajendiran Mangaiyarkarasia, Anandh Sundaramoorthy, Prakasarao Aruna, and Singaravelu Ganesan

*J. Chem. Inf. Model.*, **Just Accepted Manuscript** • DOI: 10.1021/acs.jcim.8b00558 • Publication Date (Web): 27 Nov 2018

Downloaded from <http://pubs.acs.org> on November 27, 2018

### Just Accepted

“Just Accepted” manuscripts have been peer-reviewed and accepted for publication. They are posted online prior to technical editing, formatting for publication and author proofing. The American Chemical Society provides “Just Accepted” as a service to the research community to expedite the dissemination of scientific material as soon as possible after acceptance. “Just Accepted” manuscripts appear in full in PDF format accompanied by an HTML abstract. “Just Accepted” manuscripts have been fully peer reviewed, but should not be considered the official version of record. They are citable by the Digital Object Identifier (DOI®). “Just Accepted” is an optional service offered to authors. Therefore, the “Just Accepted” Web site may not include all articles that will be published in the journal. After a manuscript is technically edited and formatted, it will be removed from the “Just Accepted” Web site and published as an ASAP article. Note that technical editing may introduce minor changes to the manuscript text and/or graphics which could affect content, and all legal disclaimers and ethical guidelines that apply to the journal pertain. ACS cannot be held responsible for errors or consequences arising from the use of information contained in these “Just Accepted” manuscripts.



## Comparative Binding Analysis of N- Acetylneuraminic Acid in Bovine Serum Albumin and Human $\alpha$ -1 Acid Glycoprotein

Subramani Karthikeyan<sup>a,b</sup>, Ganesan Bharanidharan<sup>a</sup>, Sriram Ragavan<sup>c</sup>, Saravanan Kandasamy<sup>d</sup>, Shanmugavel Chinnathambi<sup>e</sup>, Kanniyappan Udayakumar<sup>f</sup>, Rajendiran Mangaiyarkarasi<sup>a</sup>, Anandh Sundaramoorthy<sup>a</sup>, Prakasarao Aruna<sup>a</sup>, Singaravelu Ganesan<sup>a\*</sup>

<sup>a</sup> Department of Medical Physics, Anna University, Chennai-600 025, India.

<sup>b</sup> Department of Organic Chemistry, Science Faculty, Peoples' Friendship University of Russia (RUDN University), MikluhoMaklaya St.,6, Moscow, Russia, 117198

<sup>c</sup> Centre of Advanced Study in Crystallography and Biophysics, University of Madras, Chennai-600 025, India.

<sup>d</sup> Department of Physics, Periyar University, Salem-636 011 India.

<sup>e</sup> International Center for Young Scientists, National Institute for Materials Science (NIMS), 1-2-1 Sengen, Tsukuba, Ibaraki 305-0047, Japan

<sup>f</sup> Postdoctoral Research Fellow, University of Montreal, Saint – Justine Hospital University Center, 3175 Cote Sainte – Catherine, Montreal , Qc H3T1C5, Canada.

### \*Corresponding author

Dr. S. Ganesan

Department of Medical Physics

Anna University, Chennai – 600 025

Phone: +91-44-22358685

Email: [Subramanikarthikeya91@gmail.com](mailto:Subramanikarthikeya91@gmail.com), [sganesan@annauniv.edu](mailto:sganesan@annauniv.edu)

## Abstract

In this present study focus that determination of biologically significant *N*-Acetylneuraminic acid (NANA) drug binding interaction mechanism between bovine serum albumin (BSA) and human  $\alpha$ -1 acid glycoprotein (HAG) using various optical spectroscopy and computational methods. The steady state fluorescence spectroscopy result suggests that the fluorescence intensity of BSA, HAG was quenched by NANA drug in a static mode of quenching. Further time- resolved emission spectroscopy measurements confirm that mode of quenching mechanism of NANA drug in BSA and HAG system. The FT-IR, excitation - emission matrix and Circular Dichroism (CD) analysis confirms the presence of NANA drug in HAG, BSA system and fluorescence resonance energy transfer analysis shows that the NANA drug energy transfer between HAG, BSA system. The molecular docking result shows good binding affinity in both protein complex and further molecular dynamics simulations and charge distribution analysis was performed to understand more insight binding interaction mechanism of NANA drug in HAG, BSA complex.

### 1. Introduction

*N*-Acetylneuraminic acid (NANA or Neu5Ac) are widely involved in the biological activity and which is found in glycoprotein or complex of glycans on mucins at the cell membrane. NANA drug is essential for pathogenic bacteria also it can use as a nutrient by giving carbon and nitrogen atoms to the bacteria. In some cases, we found activated pathogens in the cell surface. *N*-acetylmannosamine or 6-phosphate mannose contraction caused synthesis of Neu5Ac with activated pyruvate and followed up by dephosphorylation within the cell. In several parts of glycoconjugates chains, most sialic acids are naturally originated at the terminus of *N*-glycans, *O*-glycans, and glycosphingolipids<sup>1-3</sup>.

Being at the consequence of essential cell-surface glycoconjugates, sialic acids are admirably located to arbitrate carbohydrate–protein communications in cell–cell understating phenomena. For example, sialic acids are required in the Sialyl Lewis<sup>x</sup>-selection binding that appears in the enrollment of leukocytes in the course of inflammation mechanism<sup>4</sup>. Also, sialic acids are performing as receptors for a few toxins, bacteria, and viruses. For example, the contact between Neu5 Ac and heamagglutinin add up to the primary step of infection by the influenza virus. Also, sialic acids play significant role in masking to counter the biological recognition. Alternations in sialic acids can prevent with the mechanism of cell interaction.

1  
2  
3 In this regard, it is essential to understand the binding interaction mechanism of NANA  
4 drug in both HAG and BSA molecule to explore the biochemical mechanism in a biological  
5 environment. Human  $\alpha$ -1 acid glycoprotein consists of 10 – 15 % of sialic acid residues in the  
6 total weight of the protein molecule, also it is a major plasma glycoprotein. Which contain 181  
7 amino acid residues with single polypeptide chain and the molecular weight are about 41 kDa,  
8 and it is heavily glycosylated made up of 40% of carbohydrate, 10 – 15 % of sialic acids by  
9 weight of the protein. HAG is from lipocalin protein family, and it has common structural motifs  
10 comparing its super family member. Eight anti-parallel beta sheets circularly closed by forming a  
11 barrel type structure provide a ligand binding region <sup>5-8</sup>.

12  
13  
14  
15  
16  
17  
18  
19 In other hand serum albumin also one of the primary class of transport protein, which can  
20 balance osmotic pressure and transport both exogenous, endogenous compounds. In many cases,  
21 bovine serum albumin (BSA) is considered as a model protein to perform binding analysis,  
22 because it can distribute many compounds into the particular target. BSA is a one of globular  
23 protein which consists of 583 amino residues and contains three domains (I, II, III), each as  
24 divided by subdomains A and B respectively. Also, the molecule structure contains 17 disulfide  
25 links and in both BSA, HAG protein molecule, tryptophan residue plays a major intrinsic  
26 fluorophore <sup>9</sup>.

27  
28  
29  
30  
31  
32  
33 In this context, the present study focus on the binding mechanism of NANA drug in both  
34 BSA and HAG is explained and compared by various spectroscopy techniques such as  
35 fluorescence steady-state analysis, time-resolved life time decay studies, FT-IR. The molecular  
36 docking and molecular dynamics analysis clearly explain the interaction mechanism and stability  
37 of NANA drug in both BSA, HAG protein environment. Further charge distribution analysis  
38 explores the intermolecular interaction of NANA drug in both protein molecule environments <sup>10-  
39  
40  
41  
42  
43  
44</sup>

## 45 **2. Materials and Methods**

### 46 **2.1 Materials**

47  
48 The bovine serum albumin (A2058), human  $\alpha$ -1 acid glycoprotein (G 9885) products  
49 were purchased from Sigma Aldrich, India. *N*-Acetylneuraminic acid (16091) purchased from  
50 Cayman Chemicals, USA.  
51  
52  
53  
54  
55  
56  
57  
58  
59  
60

## 2.2 Preparations of BSA, HAG and NANA solutions

All the experiments were done using a phosphate buffer solution (pH 7.2). Both protein molecules were used without any further purification. BSA and HAG protein molecules were also broadly dialyzed using in the same buffer and for both protein molecules, 1 mg/ml stock solutions prepared in the same buffer, the purity of both molecules were determined UV-visible absorption spectrophotometer (Perkin-Elmer Lambda35, Waltham, MA) at 280 nm wavelength regions. *N*-Acetylneuraminic acid (NANA) drug was dissolved using DMSO (Dimethyl sulfoxide) and stock solution was prepared (3.5 mM) using the same solvent.

## 2.3 Steady-state fluorescence quenching measurements

Fluorolog-3, ISA; Jobin-Yuvon-Spex, Edison, NJ was used to perform the emission spectral analysis of both BSA and HAG –NANA drug complex, the spectra were recorded between 280 nm – 500 nm wavelength range with 5 nm excitation, emission slit width. The emission spectrum of BSA, HAG – NANA drug complex was recorded at 298K with 280 nm excitation and the maximum emission wavelength observed at 350 nm, 347 nm respectively. The titration of BSA (10  $\mu$ M), HAG (10  $\mu$ M) and the NANA drug concentration vary from 0 to 2  $\mu$ M with 0.4  $\mu$ M for BSA complex and 0.2  $\mu$ M for HAG complex. The decreasing fluorescence intensity of BSA, HAG – NANA drug complex quenching mechanism was determined using Stern – Volmer Equation <sup>14</sup>. Also, due to the inner filter effect the following steady state spectrum must be corrected using the following equation [2]

$$F_0/F = 1+k_q\tau_0 [\text{NANA}] = 1+K_{SV} [\text{NANA}] \quad [1]$$

$$F_{\text{corr}} = F_{\text{obs}} \cdot e^{-(A_1 + A_2)/2} \quad [2]$$

Where,  $K_{SV}$  is the quenching constant,  $k_q$  rate constant of the biomolecule quenching reaction  $\tau_0$  is the average lifetime value of fluorophore (tryptophan, tyrosine) which is present in biomolecule complex and,  $F_{\text{corr}}$  and  $F_{\text{obs}}$  denote the fluorescence intensities after and before correction at the emission wavelength  $A_1$  and  $A_2$  are the total absorbance of all components at the  $\lambda_{\text{ex}}$  and  $\lambda_{\text{em}}$ , respectively<sup>50,51</sup>. In many reported literature mentioned that the average lifetime of protein molecules is in the range of 3 to 6 ns and it varies depending upon many parameters. The binding constant and number of binding sites for BSA, HAG –NANA complex were determined using double logarithmic plot equation 3 <sup>15</sup>.

$$\log [(F_0-F)/F] = \log K_b + n \log [NANA] \quad [3]$$

Where,  $F_0$  and  $F$  are the initial and final fluorescence intensities of BSA, HAG –NANA drug complex,  $K_b$  is the binding constant and  $n$  is the binding sites of protein – drug complex. Also, the free energy changes  $\Delta G^\circ$  for protein – drug complex was calculated using equation 4.

$$\log K_b = -\frac{\Delta H^\circ}{RT} + \frac{\Delta S^\circ}{R}, \Delta G^\circ = \Delta H^\circ - T \Delta S^\circ = -RT \ln K_b \quad [4]$$

Where  $T$  is the temperature (298K, 300K and 304 K),  $R$  is the gas constant (1.987 cal mol<sup>-1</sup> K<sup>-1</sup>), enthalpy ( $\Delta H^\circ$ ), entropy ( $\Delta S^\circ$ ) and free energy ( $\Delta G^\circ$ ) and  $K_b$  is the binding constant of BSA, HAG – NANA complex<sup>16-20</sup>.

#### 2.4 Time- resolved emission spectroscopy analysis (TRES)

The fluorescence lifetime measurements were carried using Time- Correlated Single Photon Counting system (TCSPC), Fluorolog – 3, HORIBA Jobin Yvon, INC, Edison, NJ. The protein molecule sample was excited using 280 nm Nano LED source (Pulse Width: < 1 ns) with rapid response red- sensitive photomultiplier (PMT; R928P, Hamamatsu Photonics, Shizuoka-Ken, Japan) detector. The fluorescence decay profile of both protein molecules was compiled at 90° from the exciting path of the light source. The obtained signal was amplified using a pulsed amplifier (TB-02, Horiba) model and delivered to the single channel fraction timing discriminator using Model No. 6915, Philips Scientific, and Mahwah, NJ. Initially detected photon was used by time to time amplitude ( $\alpha$ ) converter (TAC) until the signal peak reached 1000 counts for 350 nm emission. Using the Ludox - 40 reagents, the instrument response was obtained at 280 nm excitation wavelength region before performing the protein –drug interaction decay experiment. The obtained final output was analyzed by using Decay Analysis Software (DAS6 v6.0, Horiba) and the excellent linearity of the fitted decay profile for protein – drug complex is verified by chi – square values. The average lifetime value is calculated from the equation 5<sup>21</sup>.

$$\tau_0 = \frac{\sum_{i=1}^3 \alpha_i \tau_i^2}{\sum_{i=1}^3 \alpha_i \tau_i}$$

[5]

## 2.5 Fourier transforms infrared spectra (FTIR) analysis

The FTIR spectroscopy analysis was carried out using a JASCO instrument model no FT/IR-6600 type A series, for both protein and drug complexes. The experiment was conducted at ATR (Attenuated Total Reflectance) mode for both protein and drug complexes at room temperature 298K. The background of the sample was subtracted before performing the experimenting BSA, HAG – NANA complex. Using the instrument software the spectral noise, CO<sub>2</sub> was reduced, and base lines are corrected for all samples. The wave number ranges starts from 399.193 cm<sup>-1</sup> to 4000.6 cm<sup>-1</sup> with 0.964233 cm<sup>-1</sup> data interval at 45° incident angle for all samples, outputs were collected by Triglycine sulfate (TGS) detector system for further sample analysis<sup>17</sup>.

## 2.6 Circular Dichroism (CD) analysis

The CD analysis was carried out using JASCO instrument J-715 series for both protein and drug complexes. The concentration of both BSA and HAG is 20 μM and the NANA concentration also 20 μM range (1:1 ratio). The spectrum was recorded between 180 nm to 300 nm range for all the samples at room temperature. Further, obtained spectrum was analyzed using <http://bestsel.elte.hu/index.php> server.

## 2.7 Molecular docking studies

The crystal structure of HAG (PDB ID: 3KQ0), BSA (PDB ID: 4F5S) were obtained from the protein data bank (PDB). The compound structure of NANA drug was obtained from PubChem and further, the structure was drawn using ACD/chemsketch software. To perform molecular docking the before the compound structure should be energetically minimized, here the NANA compound structure was minimized using conjugate gradient algorithm 5000 steps which are inbuilt in Schrödinger software package 2018-3. Further, both protein molecules were optimized, and energy minimized using OPLS 2005 force field in protein preparation wizard panel. The co-crystal sites were noted before optimization of the protein molecule, and during the docking simulation the binding site grid box was set into that native structure region. Induced

1  
2  
3 fit docking panel is used to perform the molecular docking simulation for both proteins – NANA  
4 drug complex. Grid -based ligand docking with energetic (GLIDE) was used to find favorable  
5 interactions between ligand and the receptors with flexible conformations of ligand. Glide  
6 scoring function is given by the equation [6] below:  
7  
8

$$9 \quad GScore = 0.05 \times vdW + 0.15 \times Coul + Lipo + Hbond + Reward + RorB + Site \\ 10 \quad \quad \quad + hydrophobicity$$

11  
12  
13 [6]

14 Glide scoring with XP descriptor with Induced Fit Docking (IFD) rewards hydrophobic  
15 interactions in-between ligand and the receptors. IFD also reduces false positive of true ligand  
16 binder where by IFD induces side chain flexibility in the receptors. Maestro panel and pymol  
17 software is used to analysis output files <sup>22-28</sup>.  
18  
19  
20  
21  
22

## 23 **2.8 Molecular dynamics analysis**

24 Once the receptor -ligand complex was generated, it was subject to molecular simulation  
25 protocol using Desmond Schrödinger software package 2018-3 <sup>29, 30</sup>. Protein system was build  
26 involving periodic boundary condition with 10 Å<sup>3</sup> orthorhombic boxes from the center of mass  
27 with protein. TIP3P water solvation system was used as a buffer system with charged ions placed  
28 isotopically, to neutralize the Ewald charge summation of the solvated protein entity. The system  
29 was minimized with maximum iterations of 5000 steps with a gradient convergence threshold of  
30 1.0 kcal mol<sup>-1</sup> Å<sup>-1</sup>. Once the system is minimized, the system is subjected to Newtonian  
31 dynamics of the model system to evaluate energy of the system. 2ps steps were integrated to  
32 record the simulation. Six stage NPT ensemble default relaxation process was carried out before  
33 performing molecular dynamics simulation. Initially at first state solute restrained Brownian  
34 dynamics of the ensemble was carried by keeping the energy constant using NVT condition. In  
35 the second stage using Berendsen thermostat the NVT (*canonical*) ensemble was allowed to  
36 relax with respect to temperature with velocity resembling of every 1ps applied to the non-  
37 hydrogen solute sample. Subsequently, NVT ensemble was changed to NPT ensemble with  
38 Berendsenbarostat with the system kept at 1 atm pressure followed by system equilibration of  
39 1ns. Then the ensemble was subjected to 50 ns Molecular dynamics run.  
40  
41  
42  
43  
44  
45  
46  
47  
48  
49  
50  
51  
52  
53

## 54 **2.9 Density functional theory (DFT) calculation analysis**

55  
56  
57  
58  
59  
60



The best docked pose for both protein – NANA drug complexes were taken for further understand charge distribution analysis. The obtained free NANA and NANA in complex structures were converted and created as a Gaussian input file with needful geometrical parameters and basis set. After getting the docked complex, the NANA molecule is taken from the active site of both protein molecules for further DFT single point energy calculation using B3LYP/6-311G\*\* level in Gaussian 03 software package. The wave function of NANA drug in both gas phase and active regions (quantum chemical calculations) were obtained and used it for charge distribution analysis<sup>31,32</sup>.

### 3 Results and Discussion

#### 3.1 Steady- state fluorescence spectroscopy analysis

Fluorescence spectroscopy is most effective and sensitive method to understand the effect of drug binding nature in a protein molecule. There is three major fluorophore natured amino acids such as tryptophan, phenylalanine and tyrosine residues, plays a vital role in understanding protein molecule binding interaction mechanism. Among these three amino residues, tryptophan contributes more, and this can change the micro environmental surrounding of tryptophan in protein molecule. So that changes in the intrinsic fluorescence of the protein molecule can get more meaningful data and, that can be utilized to understand the conformational changes in the protein molecule. In general, the emission maxima of protein molecules obtained in 350 nm due to tryptophan residues

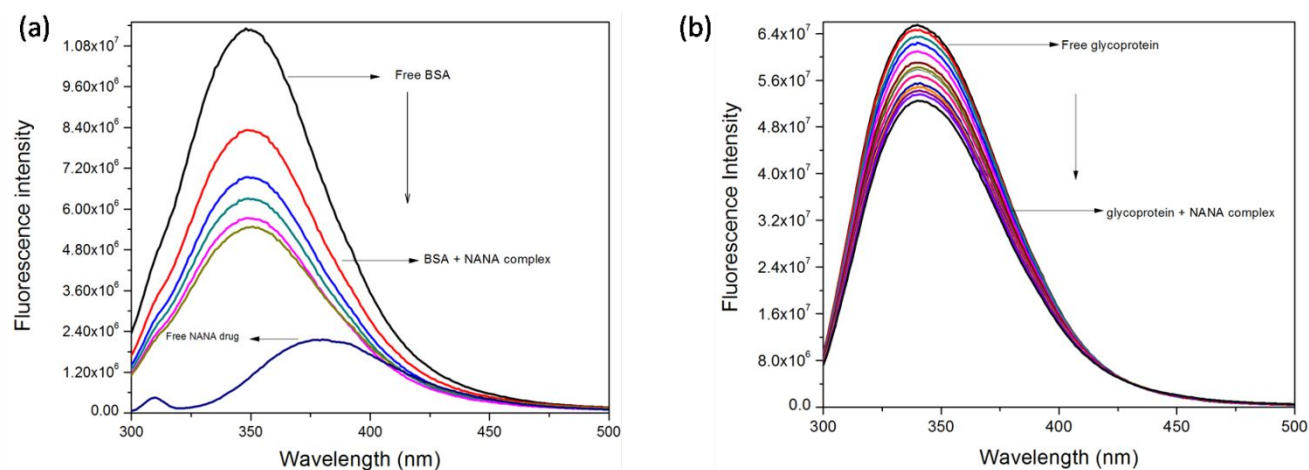


Figure 1 Steady state emission spectrum of (a) free BSA with BSA-NANA complex (b) free glycoprotein with glycoprotein – NANA complex

Figure 1 shows the steady state emission spectrum of (a) BSA – NANA complex (b) glycoprotein – NANA complex. Here both protein BSA (10  $\mu\text{M}$ ), HAG (10  $\mu\text{M}$ ) molecule kept as a control and NANA drug varies from 0 to 2  $\mu\text{M}$  with 0.2  $\mu\text{M}$  interval in HAG, 0.4  $\mu\text{M}$  interval in BSA system respectively. From the figure 1 (a) and (b) the result shows that when increasing the concentration of NANA, the fluorescence intensity of both protein molecules is decreased without any further shift, this may be due to the influence of NANA in both protein complex. This result suggests that NANA molecule may develop hydrophobicity in both BSA and HAG complex, also possibilities of deterioration in polarity around tryptophan residue due to the presence of NANA in both protein complexes. So that from this result we may conclude that NANA molecule acts the same in both the BSA and HAG protein molecule environment<sup>33</sup>.

### 3.2 Determination of quenching mechanism and binding constant

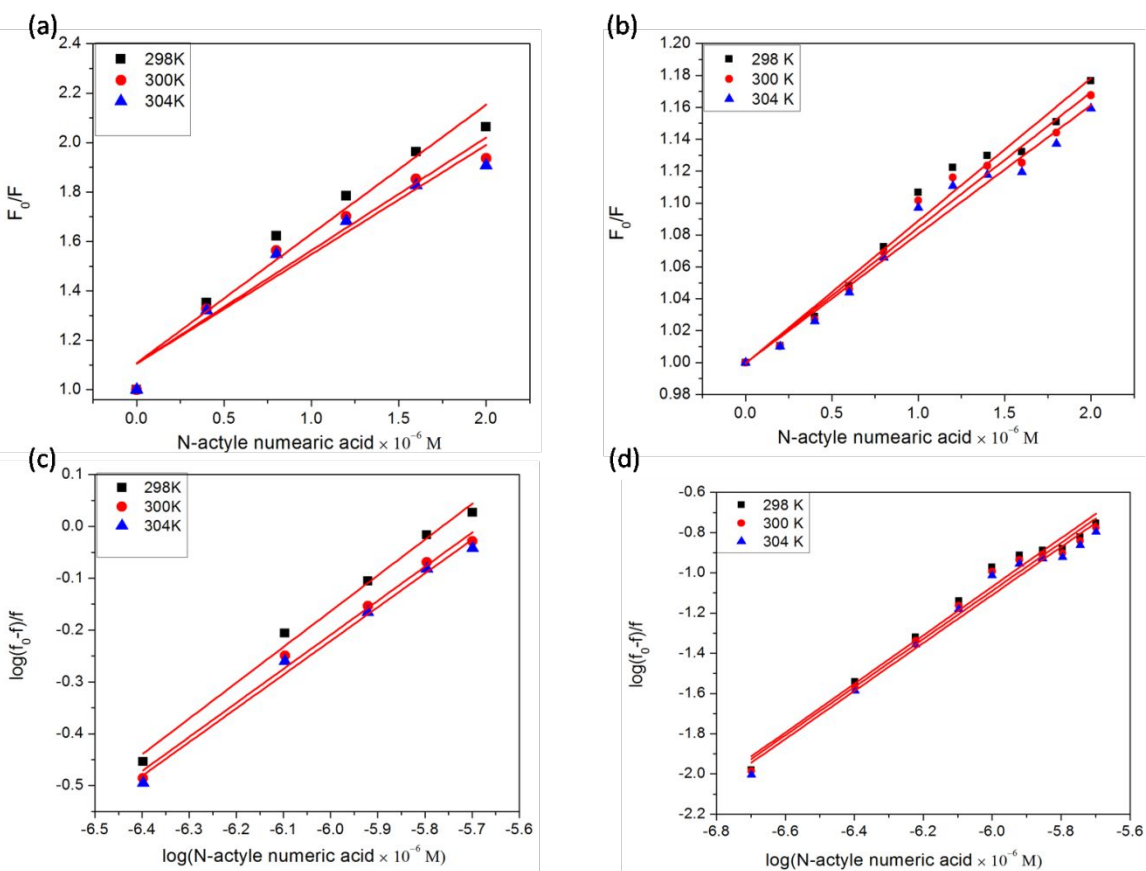


Figure 2 Stern-Volmer plot and log plot of (a) & (c) free BSA with BSA-NANA complex, (b) & (d) free glycoprotein with glycoprotein – NANA complex

The quenching fluorescence data explore the mode of binding information for NANA drug in both BSA and HAG system. In general, the fluorescence quenching is classified by two modes, one is static quenching and another one is dynamics quenching. Static quenching mode explains about the ground state complex formation between protein – drug molecule, for example before excitation occurs, but in dynamics quenching refers to after the excitation of quencher (excited state complex). Figure 2 (a) and (b) shows the Stern-Volmer plot of BSA-NANA, HAG-NANA complex system. Based on equation 1 quenching constants were calculated for both complexes (Table 1).

NANA in complex with	T(K)	$K_{SV}$ ( $\times 10^8$ L/ mol/ s)	$K_q$ ( $\times 10^{17}$ L/ mol/ s)	$K_b$ ( $\times 10^6$ L/mol)	n	$\Delta H^\circ$ (KJ/mol)	$\Delta G^\circ$ (KJ/mol)	$\Delta S^\circ$ (J/mol/K)
BSA	298	0.68	0.119	3.97	0.96	-77.90	-34.69	-149.47
	300	0.62	0.107	3.73	0.93		-34.93	
	304	0.60	0.105	3.68	0.95		-35.39	
Glycoprotein	298	8.50	2.83	6.17	1.21	-97.02	-36.72	-127.02
	300	8.10	2.70	6.08	1.19		-36.97	
	304	7.96	2.57	6.04	1.09		-37.46	

Table.1 Fluorescence binding Parameters for BSA, glycoprotein –NANA complex (pH-7.4)

The maximum scattering collision quenching constant  $K_q$ , of various quenchers with macromolecules is about  $2.0 \times 10^{10}$  L mol<sup>-1</sup> s<sup>-1</sup>. The calculated  $K_q$  values show that NANA binding mode is higher than the maximum scattering collision quenching constant of  $K_q$  and mainly due to static in nature for BSA, HAG protein molecules and also the plot shows good linearity in both complexes. Further to understand the relationship between BSA, HAG and NANA drug complex, the double logarithmic plot was plotted and shown in figure 2 (c) and (d). The binding constant for BSA – NANA complex  $K_b$  is  $3.97 \times 10^6$  L/mol but in the case of HAG –NANA complex which showing,  $K_b$  value is about  $6.17 \times 10^6$  L/mol at 298 K. Also, the binding stoichiometry for NANA in both protein molecules is almost same in the order of 1; this result reveals that the NANA can be a one class of binding in both protein molecule environments<sup>34, 35</sup>. Also, according to Ross and Subramanian theory the binding mode

1  
2  
3 association of small molecule into the protein molecule microenvironment can be divided into  
4 three sub class which is (i)  $\Delta H^\circ > 0$ ,  $\Delta S^\circ > 0$  correspond to hydrophobic forces,(ii)  $\Delta H^\circ < 0$ ,  $\Delta S^\circ$   
5  $< 0$  correspond to van der Waals interaction, hydrogen bond formation,(iii)  $\Delta H^\circ < 0$ ,  $\Delta S^\circ > 0$   
6 correspond to electrostatic interaction and the thermodynamic binding parameters of NANA in  
7 complex with BSA and HAG calculated through the van't Hoff curve (Fig S1) and  $\Delta H^\circ$ ,  $\Delta S^\circ$  and  
8  $\Delta G^\circ$  values are given in Table 1, from that result the binding force of NANA in both HSG and  
9 BSA complex mainly due to van der Waals interaction/ hydrogen bond formation<sup>51-53</sup>.

### 16 17 **3.3 Time- Resolved Emission Spectroscopy analysis (TRES)**

18  
19 Time- resolved emission measurement is a most effective method to confirm the mode of  
20 quenching in a protein molecule. The alteration in BSA, HAG protein microenvironment and  
21 conformational changes were analyzed using lifetime and its amplitude. In general, the protein  
22 molecules decay profiles were measured at 350 nm emission using 280 nm excitation LED  
23 source. But, here time resolved emission spectroscopy (TRES) method is carried between 280  
24 nm to 400 nm wavelength region with 10 nm excitation interval to understand the NANA  
25 behavior in both BSA, HAG system. Figure3 (a) and (c) shows average photon counts of TRES  
26 data of BSA – NANA, HAG – NANA complex system respectively. The average photon count  
27 plot shows that NANA drug made little impact on both protein molecule fluorophore regions  
28 without any further shift only quenching is happen between 280 nm to 400 nm wavelength  
29 region; this result concluded that presence of NANA drug in both BSA, HAG system. Further,  
30 the obtained decay amplitudes for BSA, HAG-NANA complex systems were analyzed using  
31 DAS 6.0 software and triple exponential global fitting parameter was used to extract data sets for  
32 this biomolecule. The average lifetime value  $\tau_0$  is calculated for both free protein and protein -  
33 ligand complex system and plotted wavelength versus  $\tau_0$  (Figure 3 (b) & (d)). Figure 3 b clearly  
34 shows the average photon count difference between free BSA and BSA – NANA complex,  
35 initially for 280nm wavelength there is no much difference between free BSA and BSA – NANA  
36 complex but the real difference start from 320 nm and these counts intense increases up to 360  
37 nm and saturated after that until 400 nm end wavelength region.

38  
39 The similar thing happens for free HAG and HAG – NANA (Figure 3 c) complex and  
40 these results suggest that NANA presence in both protein molecule. Figure 3 b & d shows the  
41 calculated  $\tau_0$  average life time value for free BSA, BSA – NANA complex and free HAG,  
42  
43  
44  
45  
46  
47  
48  
49  
50  
51  
52  
53  
54  
55  
56  
57  
58  
59  
60

HAG-NANA complex respectively. Figure 3b clearly shows that free BSA lifetime value starts from 1.05 ns at 280 nm and it increases towards 5.54 ns for 330 nm, after that saturated until 400 nm, but in the case of BSA- NANA complex this values is decreases to 0.118 ns for 280 nm and for 330 nm it reaches 2.54 ns and sutured after that until reaching 400 nm. In the case of free HAG the lifetime value is between 2.75 ns (350 nm) to 2.82 ns (360 nm -400 nm) and it decreases 2.66 ns (350 nm) to 2.77 ns (360 nm to 400 nm) for HAG – NANA complex. These results suggest that the NANA drug can form ground state complex in both protein molecule during the binding interaction period <sup>21, 35-36</sup>.

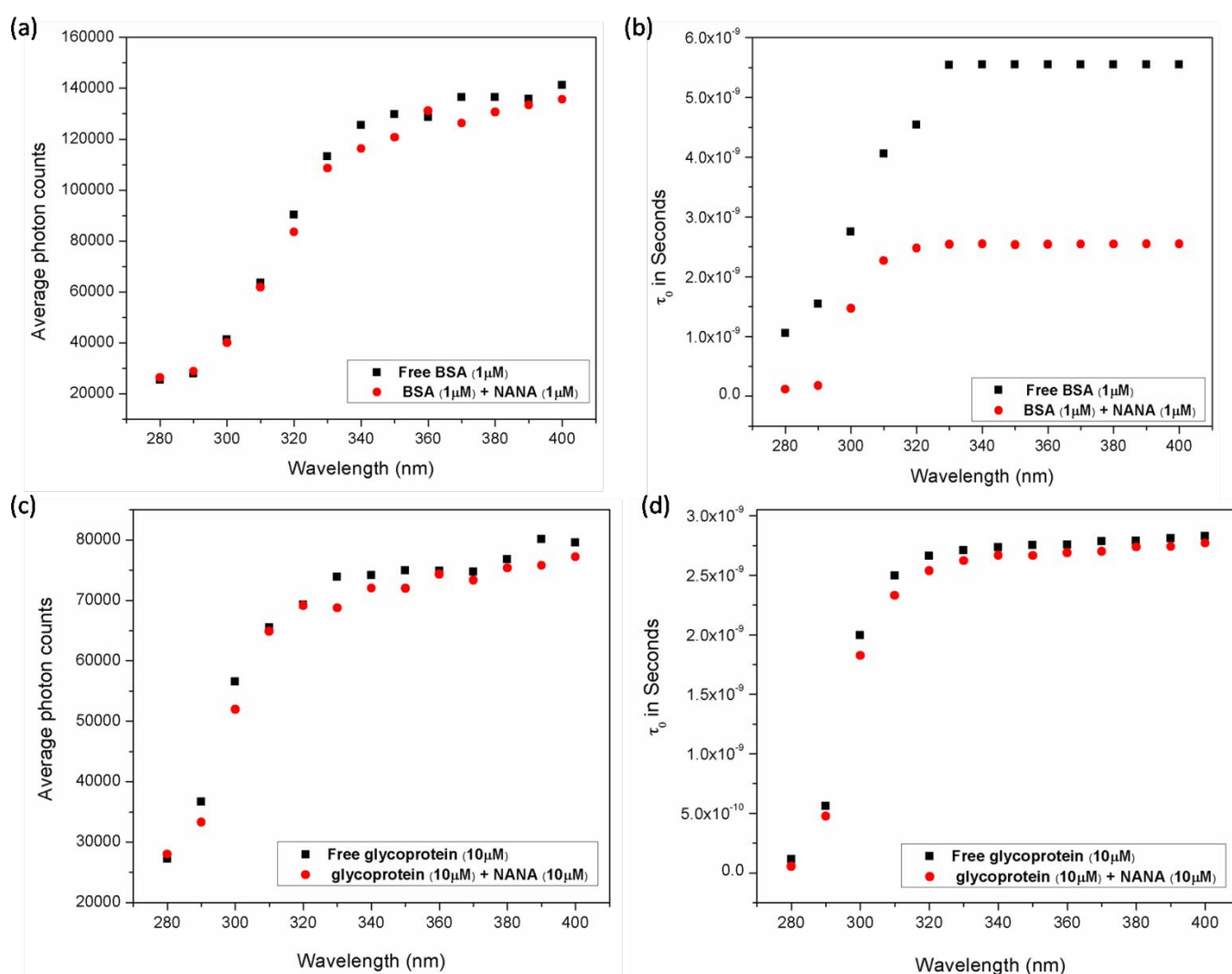


Figure 3 Time resolved emission spectroscopy analysis of (a) free BSA (b) BSA-NANA complex (c) free glycoprotein (d) glycoprotein – NANA complex

### 3.4 Forster Resonance Energy Transfer analysis (FRET)

The resonance transfer energy analysis explains the quantitative determination of transfer efficiency between donor and acceptor. The efficiency of energy transfer for NANA in both BSA and HAG (1: 1  $\mu$ M) calculated according to Forster theory using the following equation 7

$$E = 1 - \frac{F}{F_0} = \frac{R_0^6}{R_0^6 + r^6} \quad [7]$$

Where E is energy transfer efficiency,  $R_0$  is critical energy distance, r is distance and  $F_0$ , F is initial and final intensities of free BSA,HAG and BSA,HAG- NANA complex.

$R_0$  critical energy is calculated equation 8.

$$R_0^6 = 8.79 \times 10^{-25} [k^2 N^{-4} \phi_D J] \quad [8]$$

Where  $k^2 = 2/3$  is dipole spatial orientation factor,  $N = 1.336$  is a refractive index,  $\phi_D = 0.198$  is quantum yield, J is overlapping integral of donor (BSA,HAG) and acceptor of NANA molecule

$$J(\lambda) = \int_0^\infty F_D(\lambda) \epsilon_A(\lambda) \lambda^4 d\lambda \quad [9]$$

The overlapping integral is calculated using equation 9,  $F_D(\lambda)$  is donor (BSA,HAG) fluorescence intensity;  $\epsilon_A(\lambda)$  is acceptor (NANA) molar extension co-efficient.

Figure S2 (a) & (b) shows the overlap emission of BSA, HAG and absorbance of NANA spectrum, from this data integral overlapping value is calculated for both molecule and calculated J is  $1.902 \times 10^{-21}$   $\text{cm}^3 \text{L/mol}$  for BSA -NANA and  $6.809 \times 10^{-21}$   $\text{cm}^3 \text{L/mol}$  for HAG-NANA. The  $R_0$  also calculated from above equation 6 which 1.78 nm for BSA- NANA complex and 2.31 nm for HAG-NANA complex. The efficiency E for BSA – NANA is 0.0601 and for HAG – NANA is 0.0234. The final distance r is 3.1 nm for BSA-NANA and 4.3 nm for HAG – NANA. Since, the average reported distance r value is  $< 7\text{nm}$ . Hence, from the above calculated result suggests that NANA drug is within the binding region and possibilities of energy transfer for both BSA and HAG molecule <sup>16-18,55</sup>.

### 3.5 Excitation emission matrix analysis

The excitation emission matrix analysis clearly explains about the presence and absence of NANA drug and conformational changes in both BSA, HAG microenvironment. The three dimensional fluorescence spectral data of free BSA (Fig S3a), BSA – NANA (Fig S3b) and free HAG (Fig S3c), HAG – NANA (Fig S3d) complex is shown in figure S3. The concentration of both protein and NANA molecule here kept as 1: 1  $\mu\text{M}$ . In three dimensional panels, the excitation range was set into 230 nm to 700 nm with 10 nm intervals and emission was 2 nm integral with 5 nm bandpass filter for both excitation emission. From the figure S3a and S3b there is no shift and the new peak is observed, but the emission maxima are decreased for BSA – NANA complex comparing with free BSA, this result suggests that presence of NANA in BSA molecule and this result similar to the free HAG, HAG –NANA complex also. The overall result concludes that NANA drug forms a complex and rearrange the native structure of both protein molecule hydrophobic binding cavity<sup>17,56,58</sup>.

### 3.6 FT-IR analysis

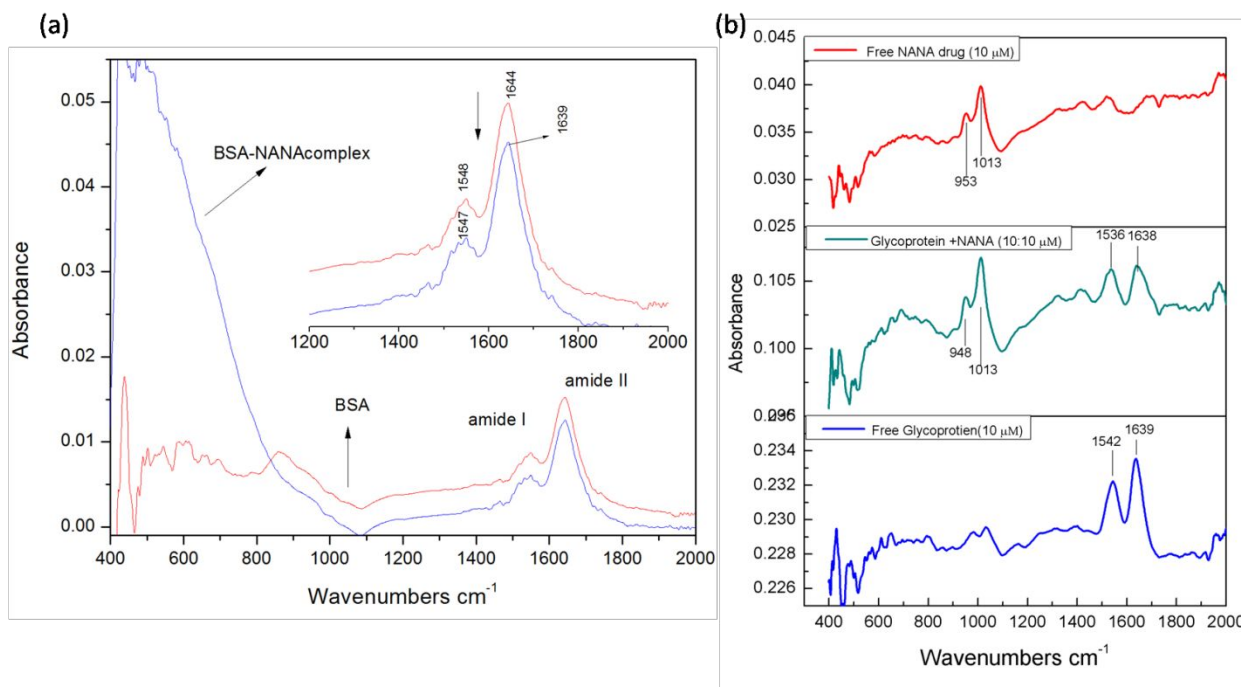


Figure 4 FT-IR spectrum of (a) free BSA with BSA-NANA complex (b) free glycoprotein with glycoprotein – NANA complex

1  
2  
3  
4  
5  
6  
7  
8  
9  
10  
11  
12  
13  
14  
15  
16  
17  
18  
19  
20  
21  
22  
23  
24  
25  
26  
27  
28  
29  
30  
31  
32  
33  
34  
35  
36  
37  
38  
39  
40  
41  
42  
43  
44  
45  
46  
47  
48  
49  
50  
51  
52  
53  
54  
55  
56  
57  
58  
59  
60

FT-IR spectroscopy technique is used to understand the conformational changes in BSA and HAG, and also to explore the effect of NANA drug in both protein molecule environments. Figure 4 (a) & (b) shows free BSA and BSA –NANA complex, free HAG and HAG – NANA complex respectively. In general for the protein molecules amide peaks will be in the region of  $1500 - 1700 \text{ cm}^{-1}$  due to C=O stretch and N-H bend in the protein peptides. Also the amide I band (C- N stretch) is more sensitive while comparing with amide II band (C-N stretch, N-H bend). Here both protein and drug molecule are kept 10:10  $\mu\text{M}$  ratio at 298K. Figure 4a shows the absorbance spectrum of free BSA molecule and the amide I and II bands are observed at  $1548 \text{ cm}^{-1}$  and  $1648 \text{ cm}^{-1}$  respectively.

While adding the NANA drug, the absorbance intensity is decreased and slight lower wavelength region shift is occurs in the amide II ( $1547 \text{ cm}^{-1}$ ) and amide I ( $1639 \text{ cm}^{-1}$ ) which confirms the presence of NANA in BSA microenvironment. On the other hand figure 4 b shows a similar effect of NANA in HAG microenvironment. From this overall result suggest that NANA could able to bind in both protein molecule and there is a possibility of structural rearrangements in NANA binding region <sup>17-18, 37,57</sup>.

### 3.7 CD analysis

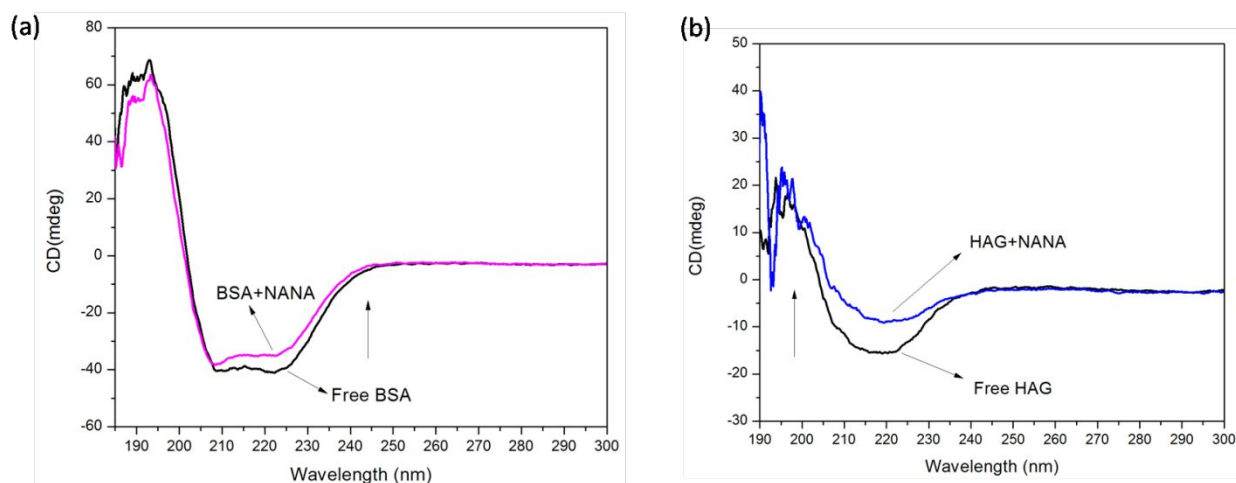


Figure 5 CD spectrum of (a) BSA-NANA system (b) HAG-NANA system



The CD analysis was performed to understand the secondary structural conformation in both BSA, HAG in NANA complex. Fig 5 (a) and (b) clearly shows the difference between free BSA, HAG and BSA, HAG with NANA complex. From that Fig 5a shows two negative bands between 208 nm and 222 nm wavelength region due to the alpha helix but in the case of Fig 5b shows one negative band mainly due to the presence of beta strands. Also, to NANA in both BSA and HAG system shows that notable increase and slight shift. It is mainly due to the presence of NANA in both protein molecular secondary structural elements (SSE) (alpha helix (BSA), beta strands (HAG)) loss in their stability or it may re-arranged in total the orientation of total secondary structural elements. Also, the calculated SSE is shown in table S2 and the experimentally obtained result also compared with MD SSE analysis shown in Fig S7 (BSA-NANA) S8 (HAG –NANA) and the overall result suggest that the presence of NANA in BSA and HAG SSE of both protein molecule may partially unfold or re-oriented<sup>53,54,59</sup>.

### 3.7 Molecular docking analysis

The molecular docking studies were performed to understand more about the NANA binding insight mechanism in both BSA and HAG molecule. The above experiment section may confirm the NANA drug presence in both BSA and HAG, but in molecular docking results reveals the specific interaction mechanism of NANA in two essential protein molecules. Figure S4 (a), (b) & (c) shows the best binding pose of NANA in BSA and its inset shows binding position, also interacting active site residues. Similarly, Figure S4 (d), (e) & (f) shows the best binding complex of NANA in HAG, inset is respective binding position and finally NANA interacting active site residues in HAG environment. The NANA molecule forms five hydrogen bonding interaction with (ASN 404, TYR 400, LYS 524, MET 547) BSA microenvironment with four amino acid residues (Figure S4c) , but in the case of HAG complex NANA drug forming seven hydrogen bonds with six amino acid (TYR 127, ARG 90, THR 47, GLU 64, TYR 27, SER 125) residues (Figure S4f). Interestingly the tyrosine residues were in active site region in both NANA – protein complexes, this residue is one of the significant fluorophore in the fluorescence study and this results may value added to the fluorescence spectroscopy results for confirmation of the presence of NANA in both protein complex. Also, based on the binding energy, the best docked poses were taken for BSA- NANA and HAG-NANA complex.

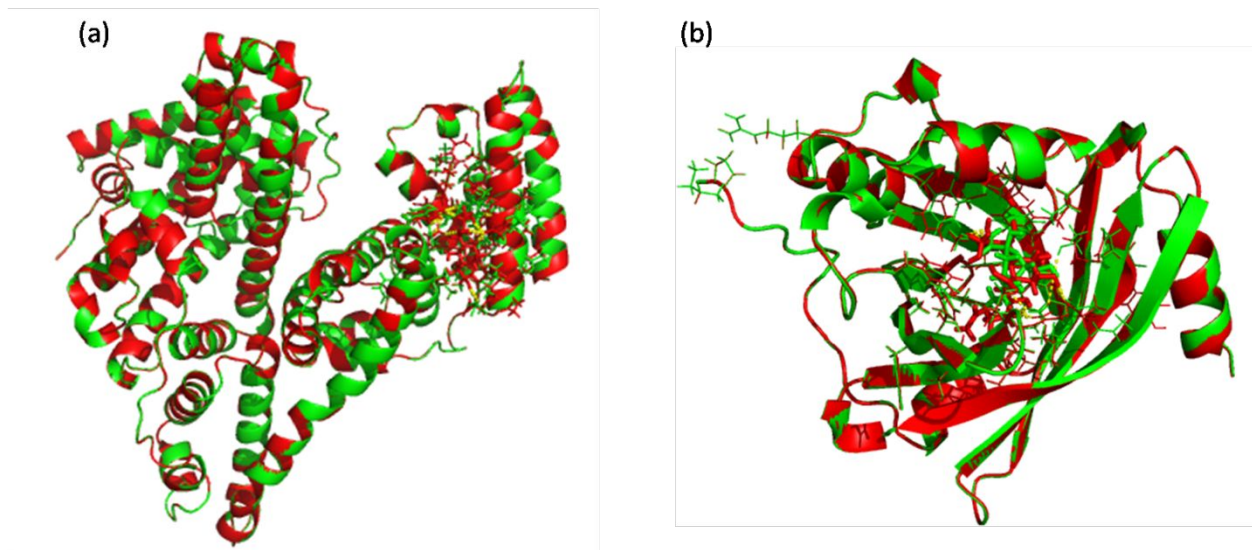


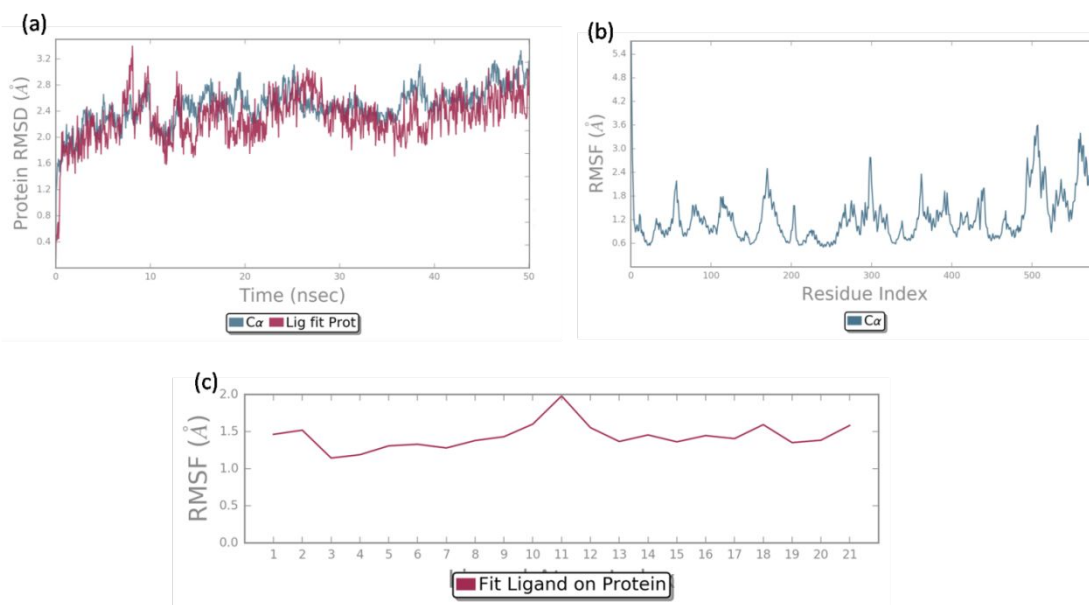
Figure 6 shows the superimposed structure of initial (green) and final (red) MD outputs of (a) BSA – NANA complex (b) HAG –NANA complex

The calculated binding energy for BSA –NANA is -48.93 KJ/mol and -44.38 KJ/mol for HAG –NANA complex among 20 different binding scores. Based on equation 3 the obtained docking scores were compared with experimental and theoretical data. From that the for BSA – NANA complex theoretically obtained docking score is -48.93 KJ/mol and -44.38 KJ/mol is almost in the same order and this results again giving concrete evidence for fluorescence experimental studies<sup>38,39</sup>.

### 3.8 Molecular dynamics analysis

The molecular dynamics study was performed after the molecular docking to understand more about the NANA stability in both BSA and HAG system (Figure 6). In general, the dynamics studies were performed at aqueous medium at drug binding in the region of a protein molecule to understand the effect of the drug in structural level. Root mean square deviation (RMSD) data is mainly used to obtain conformational changes in the protein – ligand complex. Figure 7 (a) shows the RMSD plot of BSA – NANA complex system and the simulations were performed up to 50 ns. The figures represent the stability of NANA in a protein molecule environment and there is no much fluctuation in the secondary structure of the BSA during the

1  
2  
3 interaction session of NANA. Figure 7 (b) & (c) shows the BSA and NANA root mean square  
4 fluctuation plot, from that the backbone of protein molecule  $C\alpha$  is observed and ligand RMSF  
5 gives the information about insights of NANA fragments in BSA binding environment, and this  
6 result suggests that the due to binding impact of NANA, the BSA secondary structural region  
7 may be rearranged during the molecular dynamics simulation process. In Figure 8 (a) shows the  
8 NANA –HAG system of RMSD and these result shows that NANA drug balanced after reaching  
9 10 ns and the HAG secondary structure  $C\alpha$  also explore the same result.  
10  
11  
12  
13  
14  
15  
16  
17



18  
19  
20  
21  
22  
23  
24  
25  
26  
27  
28  
29  
30  
31  
32  
33  
34  
35  
36  
37  
38 Figure 7 Molecular dynamics simulation of BSA – NANA complex (a)RMSD (b) RMSF  
39 of BSA (c) RMSF of NANA in fitting BSA  
40  
41  
42

43 The RMSF of HAG – NANA system (Figure7 (b) & (c)) result shows that HAG does not  
44 affect the backbone of HAG during the MD simulation and this effect similar to BSA system  
45 also. The figure 7 and 8 results conclude that the binding of NANA did not affect C -alpha of  
46 both protein molecules. Figure S5 (a) and (b) shows the protein –ligand contacts of BSA –  
47 NANA, HAG-NANA respectively.  
48  
49  
50  
51  
52  
53  
54  
55  
56  
57  
58  
59  
60

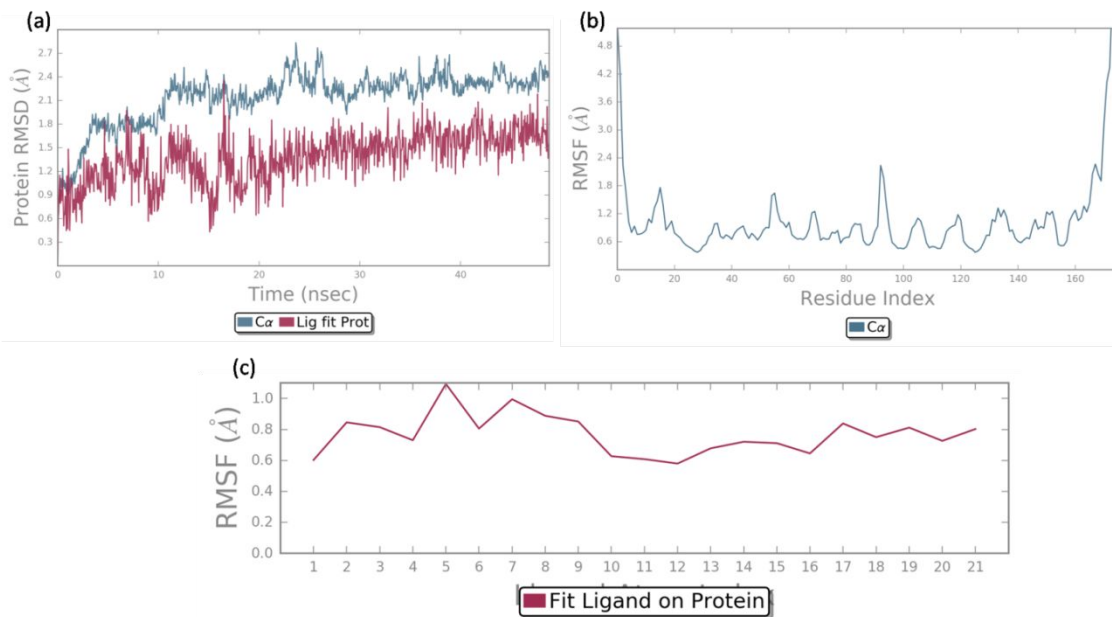


Figure 8 Molecular dynamics simulation of glycoprotein – NANA complex (a)RMSD (b) RMSF of glycoprotein (c) RMSF of NANA in fitting glycoprotein

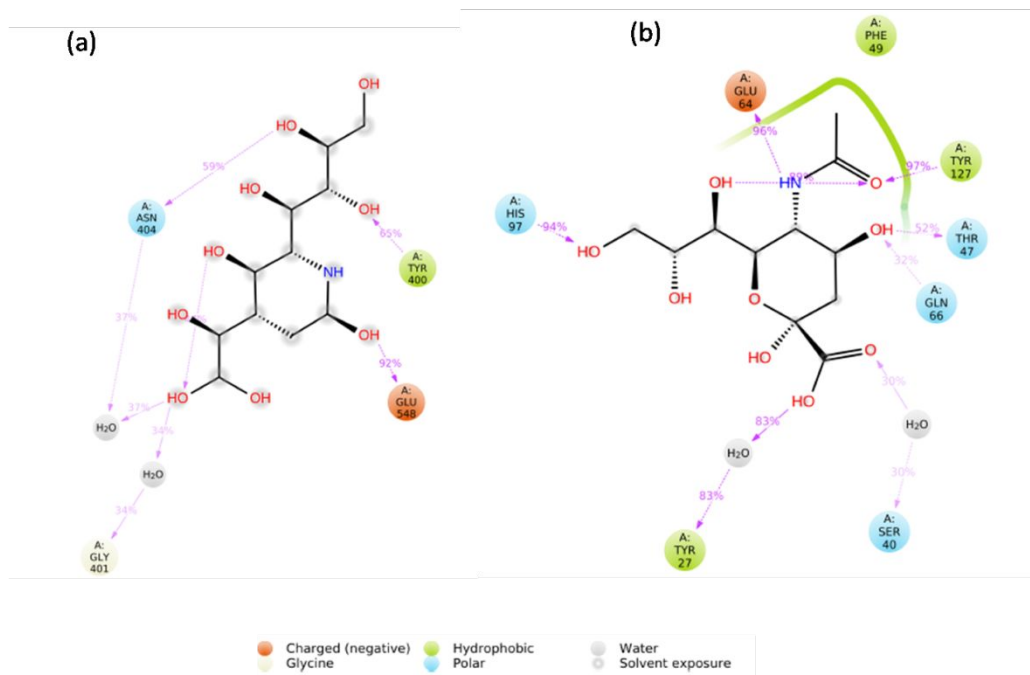


Figure 9 shows the after the simulation binding interaction plot of NANA in complex with (a) BSA (b) HAG

1  
2  
3 The active site residues were monitored throughout the simulation process from those  
4 hydrogen bonds, hydrophobic, ionic and water bridges contact were observed for NANA in both  
5 protein molecule environments. Comparing with all other active site residues tyrosine have more  
6 contacts with NANA in both protein molecules (Figure 9), around 70% of H-bond contact and  
7 20% of water bridge in BSA microenvironment (TYR 400) and in HAG TYR 27 give 90% of  
8 water bridge, TYR 127 contributes 97% of H-bond with NANA molecule.  
9

10  
11  
12  
13 Further figure S6 (a) and (b) shows the H-bond stability of BSA- NANA and HAG –  
14 NANA active site region. This result also value added for TYR residues stability for both protein  
15 molecule active site NANA microenvironment and hence this may be comparable with  
16 fluorescence results, but the molecular dynamics result concludes that NANA can be bind into  
17 both protein molecule environment. In addition to this to know the secondary structural elements  
18 (SSE) of both BSA, HAG in NANA complex is also monitored and shown in figures S7 &S8.  
19 Also, looking at the histogram and torsion profile (figure S9 & S10) may give more insights into  
20 the conformational strain of NANA in BSA, HAG complex<sup>40-42</sup>.  
21  
22  
23  
24  
25  
26  
27  
28

### 29 **3.9 Atomic charges and dipole moment analysis**

30  
31 After the docking simulation of BSA- NAN and HAG- NANA complex, there is one  
32 more possibility to understand about charge distribution analysis of NANA in both protein  
33 molecules binding site environment. Mullikan charge distribution analysis (table S1) can reveal  
34 the information of NANA molecule charge distribution environment in gas phase (free NANA)  
35 and in both BSA, HAG active site (single point) position. Form the calculated Mullikan values it  
36 is observed that most of the carbon and hydrogen atoms are positive value due to high electro  
37 negativity which is mostly bonded with oxygen and nitrogen atom. Similarly, the NANA  
38 molecule in both protein molecule active site environment reflects the same result with slight  
39 integer changes because of inter molecule interaction in both protein molecule active site region.  
40 Further, the dipole moment of NANA was also calculated to understand about polarity in protein  
41 environment and shown in figure S11. For free NANA the dipole moment was 4.51D and which  
42 is increased 4.71D for BSA active site region and 4.80D for HAG active region and this result  
43 concludes that NANA molecule could redistribute structurally as well as geometrically in both  
44 protein molecule environment<sup>43,44</sup>.  
45  
46  
47  
48  
49  
50  
51  
52  
53  
54  
55  
56  
57  
58  
59  
60

### 3.10 Electrostatic potential and frontier molecular orbital analysis

To understand the reactive site of NANA in both protein molecules the electrostatic potential analysis was done. In general from the potential map a positive atom contains electrophilic sites and negative atoms are nucleophile selectivity. Figure 10 shows the electrostatic potential map for (a) NANA, (b) BSA –NANA active site and (c) HAG – NANA active site region. From the figure10 (a) it is observed that carbon –oxygen bounded region are more nucleophile and other hydrogen atoms regions were surrounded by electrophilicity. Figure 10 (b) and (c) explains about that positive potential regions attract more amino acid residues instead of negative potential and this result suggests that NANA could form the intermolecular interaction between both protein molecular environments.

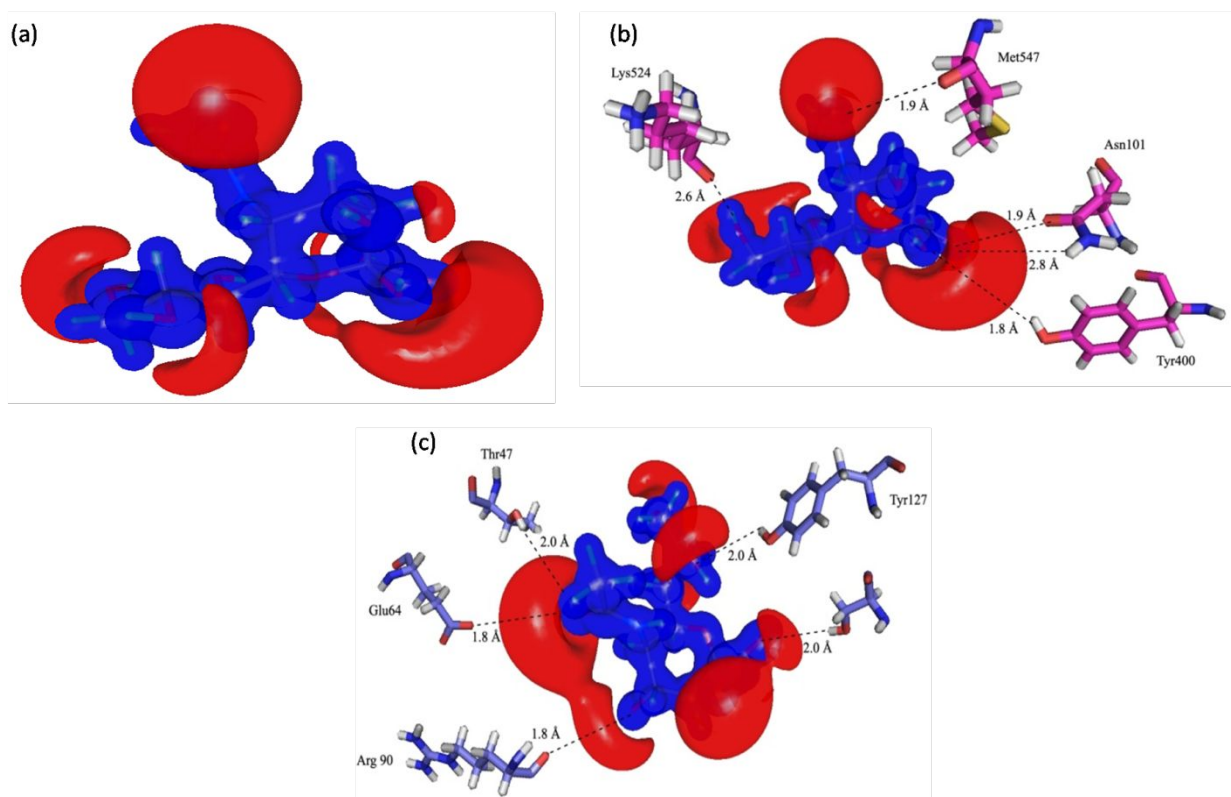


Figure 10 The molecular electrostatic potential of both molecules in isosurface representation with amino acid interactions are shown in pictorially [Blue: positive potential and Red: negative potential]. The surface values are  $+0.5$  and  $-0.05 \text{ e}\text{\AA}^{-1}$

Figure S12 shows the HOMO – LUMO molecular orbital maps of (a) NANA (b) NANA in BSA and (c) NANA in HAG complex system. This result can suggest that electron donor acceptor of highest and lowest molecular orbital during the chemical reaction. The global reactive parameters of NANA molecule calculate and shown in Table 2. The overall result concludes that NANA could form strong intermolecular interaction during the binding of both protein molecules <sup>45 – 49</sup>.

Global Reactivity Descriptors	DFT-I Energy (eV)
Band Gap	-5.45
HOMO Energy	-5.84
LUMO Energy	-0.39
Ionization Potential $I = -E_{\text{HOMO}}$	5.84
Electron Affinity $A = -E_{\text{LUMO}}$	0.39
Global Hardness $\eta = (I - A)/2$	2.73
Electronegativity $\chi = (I + A)/2$	3.12
Electrophilicity $\omega = \mu^2/2\eta, \mu = -\chi$	1.78

Table 2 The calculated global reactivity properties of NANA

#### 4. Conclusion

In summary, the overall results obtained by different techniques suggest that NANA molecule binds well in both BSA and HAG molecules. In fluorescence technique confirms the nature of quenching of NANA is a static mode in both molecule and time resolved analysis confirm that the presence of NANA in both protein molecule was stable in full wavelength region. Energy transfer analysis suggests that there is a possibility to occur between NANA and BSA, HAG and calculate r values are 3.1nm, 4.3nm respectively. The excitation emission matrix analysis, FT-IR and CD report suggest that NANA could bind BSA and HAG without disturbing

1  
2  
3 both protein native structures. Molecular docking analysis clearly shows the evidence of NANA  
4 binding in both BSA and HAG molecule also, the calculated docking is almost in the same order  
5 of experimental value again this result makes a bridge between experimental results. Further  
6 molecular dynamics simulation concludes that NANA molecule could bind without altering the  
7 native structures of the both protein molecule. The charge distribution analysis provides detailed  
8 insights and intermolecular interaction of NANA in both protein molecule environments. These  
9 types of results will improve more in future drug design and these feedbacks will help to design  
10 some new effective drugs.  
11  
12  
13  
14  
15  
16  
17  
18

### 19 **Acknowledgments**

20 Thanks to DST-PURSE (M.H.No. 7.1.3.69) phase 2 programs for providing chemical funds to  
21 Department of Medical Physics, Anna University, Chennai – 600 025. This study was also  
22 supported by the Board of Research in Nuclear Sciences, Department of Atomic Energy,  
23 Government of India, Project no.2009/34/38/BRNS/3206. The authors are thankful to Centre for  
24 Research, Anna University, Chennai for offering Anna Centenary Fellowship (Lr. No.  
25 CRF/ACRF/ Jan. 2015/36) to Subramani Karthikeyan, Department of Medical Physics, Anna  
26 University, Chennai-600 025. The publication was also prepared with the support of the “RUDN  
27 University Program 5-100.  
28  
29  
30  
31  
32  
33  
34  
35

### 36 **Conflict of Interest:**

37 There are no conflicts to declare  
38  
39  
40

### 41 **Supporting information:**

42 Supplementary materials are provided that describe more detailed information on Plots of  $\ln K_b$   
43 versus  $1/T$  for NANA binding to (a) BSA (b) HAG, FRET analysis of (a) free BSA with BSA-  
44 NANA complex (b) free glycoprotein with glycoprotein – NANA complex, Excitation Emission  
45 matrix analysis of (a) free BSA (b) BSA-NANA complex (c) free glycoprotein (d) glycoprotein –  
46 NANA complex, Pymol view of (a) BSA- NANA complex (b) inset of BSA-NANA complex (c)  
47 ligplot of BSA –NANA complex (d) glycoprotein – NANA complex (e) inset of glycoprotein –  
48 NANA complex (f) ligplot of glycoprotein – NANA complex, Interaction fraction of (a)BSA –  
49 NANA complex (b) glycoprotein – NANA complex, protein – ligand contacts during simulation  
50  
51  
52  
53  
54  
55  
56  
57  
58  
59  
60



(a)BSA –NANA complex (b) glycoprotein – NANA complex, Table of Mullikan population analysis of NANA compound complex with BSA and HAG, The BSA and HAG secondary structural elements (SSE) reports, NANA torsion profile during simulation with BSA and HAG, dipole moment vectors of NANA in both molecules in gas phase and in the binding site of BSA and glycoprotein, HOMO and LUMO of NANA and NANA in molecules were plotted at the isosurface value at 0.02 au

## Reference

1. Schauer, R.. Sialic Acids: Chemistry, Metabolism and Function; Springer Vienna–New York, 1982; Vol. 10, pp 5-50.
2. Rosenberg, A. Ed.; Biology of Sialic Acids; Plenum Press: New York, London, 1995;pp 197 -241.
3. Varki, A. Biological Roles of Oligosaccharides: All of the theories are correct. *Glycobiol.* **1993**, 3, 97–130.
4. Reutter, W.; Kottgen, E.; Bauer, C.; Gerok, W. In Sialic Acids. Chemistry, Metabolism and Function; Schauer, R., Ed.; Springer Vienna–New York, 1982; pp 263–305.
5. Herrler, G.; Hausmann, J.; Klenk, H. D. In Biology of The Sialic Acids; Rosenberg, A., Ed.; Plenum Press: New York and London, **1995**,315–336.
6. Paulson, J. C.; Colley, K. J. Glycosyltransferases. Structure, Localization, and Control of Cell type-Specific Glycosylation. *J. Biol. Chem.***1989**, 264, 17615–17618.
7. Van den Eijnden, D. H.; Joziase, D. H. Enzymes Associated with Glycosylation. *Curr. Opin. Struct. Biol.***1993**, 3, 711–721.
8. Dente, L.; Pizza, M. G.; Metspalu, A.; Cortese, R. Structure and Expression of the Genes Coding for Human Alpha 1-acid Glycoprotein. *Euro. Mol. Biol. Org. J.***1987**, 6, 2289.
9. Sitar, M. E.; Aydin, S.; Cakatay, U. Human Serum Albumin and its Relation with Oxidative Stress. *Clin. Lab.***2013**, 59, 945–952.

- 1  
2  
3 10. Paul, B. K.; Ghosh, N.; Mukherjee, S. Interplay of Multiple Interaction Forces: Binding  
4 of Norfloxacin to Human Serum Albumin. *J. Phys. Chem. B*. **2015**, 119, 13093–13102.  
5  
6  
7 11. Il'ichev, Y. V.; Perry, J. L.; Simon, J. D. Interaction of Ochratoxin A with Human Serum  
8 Albumin. Preferential Binding of the Dianion and pH Effects. *J. Phys. Chem.*  
9 *B*, **2002**, 106, 452–459.  
10  
11  
12 12. Sasmal, M.; Bhowmick, R.; Islam, A. S. M.; Bhuiya, S.; Das, S.; Ali, M. Domain-Specific  
13 Association of a Phenanthrene–Pyrene-Based Synthetic Fluorescent Probe with Bovine  
14 Serum Albumin: Spectroscopic and Molecular Docking Analysis. *ACS Omega*. **2018**, 3,  
15 6293–6304.  
16  
17  
18 13. Bourassa, P.; Kanakis, C. D.; Tarantilis, P.; Pollissiou, M.G.; Tajmir-Riahi, H.  
19 A. Resveratrol, Genistein, and Curcumin Bind Bovine Serum Albumin. *J. Phys. Chem.*  
20 *B*. **2010**, 114, 3348–3354.  
21  
22  
23 14. Tang, J.; Luan, F.; Chen, X. Binding Analysis of glycyrrhetic acid to Human Serum  
24 Albumin: Fluorescence Spectroscopy, FTIR, and Molecular Modeling. *Bioorg. Med.*  
25 *Chem*. **2006**, 14, 3210–3217.  
26  
27  
28 15. Karthikeyan, S.; Chinnathambi, S.; Kannan, A.; Rajakumar, P.; Velmurugan,  
29 D.; Bharanidharan, G.; Aruna, P.; Ganesan, S. Investigation of Optical Spectroscopic  
30 and Computational Binding Mode of Bovine Serum Albumin with 1, 4-Bis ((4-  
31 Heptylpiperazin-1-yl) Methyl)-1H-1, 2, 3-Triazol-1-yl) Methyl) Benzene. *J.*  
32 *BiochemMolecular Toxicology*. **2015**, 29, 373–381.  
33  
34  
35 16. Karthikeyan, S.; Chinnathambi, S.; Velmurugan, D.; Bharanidharan, G.; Ganesan,  
36 S. Insights into the Binding of 3-(1-Phenylsulfonyl- 2-methylindol-3-ylcarbonyl)  
37 Propanoic Acid to Bovine Serum  
38 Albumin: Spectroscopy and Molecular Modelling Studies. *Nano Biomed Eng*. **2015**, 7, 1-  
39 7.  
40  
41  
42 17. Karthikeyan, S.; Bharanidharan, G.; Mani, K. A.; Srinivasan, N. S.; Keshewani, M.;  
43 Velmurugan, D.; Aruna, P.; Ganesan, S. Determination on the binding of thiadiazole  
44  
45  
46  
47  
48  
49  
50  
51  
52  
53  
54  
55  
56  
57  
58  
59  
60

- 1  
2  
3 derivative to human serum albumin: A Spectroscopy and computational Approach. *J.*  
4 *Biomol StructDyn.* **2017**, 35, 817-828.  
5  
6  
7  
8 18. Karthikeyan, S, Bharanidharan, G.; Mani, K. A.; Srinivasan, N. S.; Keshewani, M.;  
9 Velmurugan, D.; Aruna, P.; Ganesan, S. Insights into the binding of thiosemicarbazone  
10 derivatives with human serum albumin: spectroscopy and molecular modelling studies. *J.*  
11 *Biomol Struct Dyn.* **2016**, 34, 1264-1281.  
12  
13  
14  
15 19. Shareef, M. A.; Musthafa, M.; Velmurugan, D.; Karthikeyan, S.; Ganesan, S.; Padusha,  
16 S. A.; Musthafa, S.; Mohamed. S. Synthesis, characterization, anticancer activity, optical  
17 spectroscopic and docking studies of novel thiophene-2-carboxaldehyde derivatives. *J.*  
18 *Eur.J.Chemistry.* **2016**, 7, 454-462.  
19  
20  
21  
22  
23 20. Chinnathambi, S.; Karthikeyan, S.; Keshewani, M.; Velmurugan, D.; Hanagata,  
24 N. Underlying the Mechanism of 5-Fluorouracil and Human Serum Albumin Interaction:  
25 A Biophysical Study. *J. Phys. Chem Biophys.* **2016**, 6, 2161-0398.  
26  
27  
28  
29 21. Karthikeyan, S.; Bharanidharan, G.; Mangaiyarkarasi, R.; Chinnathambi, S.; Sriram, R.;  
30 Gunasekaran, K.; Saravanan, K.; Gopikrishnan, M.; Aruna, P.; Ganesan, S. A  
31 Cytotoxicity, optical spectroscopy and computational binding analysis of 4-[3-acetyl-5-  
32 (acetylamino)-2-methyl- 2,3-dihydro-1,3,4-thiadiazole-2-yl]phenyl benzoate in calf  
33 thymus DNA. *Luminescence* **2018**, 33, 731-741.  
34  
35  
36  
37  
38 22. Friesner, R. A.; Murphy, R. B.; Repasky, M. P.; Frye, L. L.; Greenwood, J. R.;  
39 Halgren, T. A.; Sanschagrin, P. C.; Mainz, D. T. Extra Precision Glide: Docking and  
40 Scoring Incorporating a Model of Hydrophobic Enclosure for Protein-Ligand  
41 Complexes. *J. Med. Chem.* **2006**, 49, 6177-6196.  
42  
43  
44  
45  
46 23. Halgren, T. A.; Murphy, R. B.; Friesner, R. A.; Beard, H. S.; Frye, L. L.; Pollard, W. T.;  
47 Banks, J. L. Glide: A New Approach for Rapid, Accurate Docking and Scoring. 2.  
48 Enrichment Factors in Database Screening. *J. Med. Chem.* **2004**, 47, 1750-1759.  
49  
50  
51  
52 24. Friesner, R. A.; Banks, J. L.; Murphy, R. B.; Halgren, T. A.; Klicic, J. J.; Mainz, D. T.;  
53 Repasky, M. P.; Knoll, E. H.; Shaw, D. E.; Shelley, M.; Perry, J. K.; Francis, P.; Shenkin,  
54  
55  
56  
57  
58  
59  
60

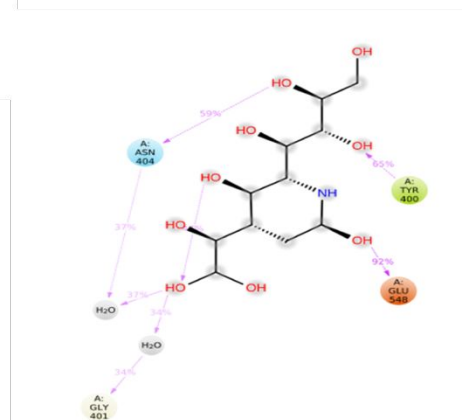
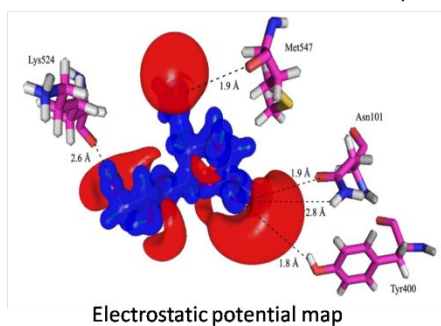
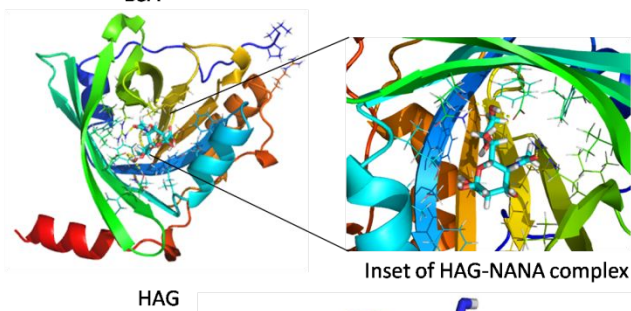
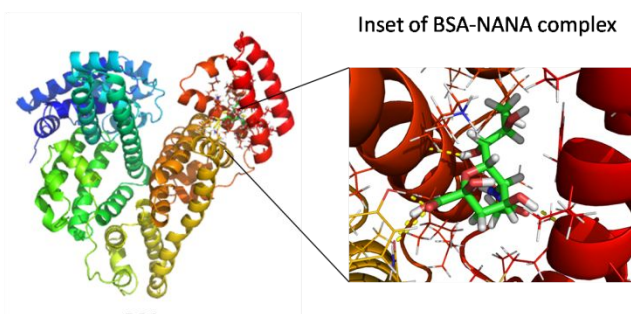
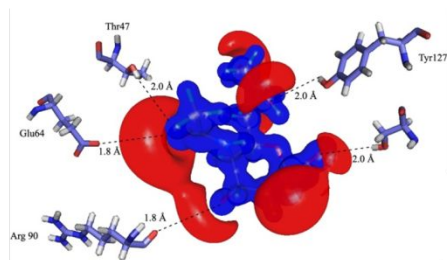
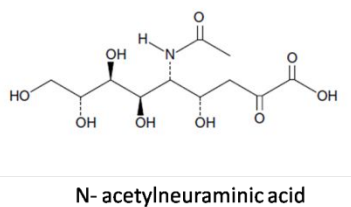
- 1  
2  
3 P. S.Glide: A New Approach for Rapid, Accurate Docking and Scoring. 1. Method and  
4 Assessment of Docking Accuracy. *J. Med. Chem.* **2004**, 47, 1739–1749.  
5  
6  
7  
8 25. Farid, R.; Day, T.; Friesner, R. A.; Pearlstein, R. A. New insights about HERG blockade  
9 obtained from protein modeling, potential energy mapping, and docking studies. *Bioorg.*  
10 *& Med. Chem.* **2006**, 14, 3160-3173.  
11  
12  
13 26. Sherman, W.; Day, T.; Jacobson, M. P.; Friesner, R. A.; Farid, R. Novel Procedure for  
14 Modeling Ligand/Receptor Induced Fit Effects. *J. Med. Chem.* **2006**, 49, 534-553.  
15  
16  
17 27. Sherman, W.; Beard, H. S.; Farid, R. Use of an Induced Fit Receptor Structure in Virtual  
18 Screening. *Chem. BiolDrug Des.* **2006**, 67, 83-84.  
19  
20  
21  
22 28. Biologics Suite 2018-2, Schrödinger, LLC, **2018**, New York, NY, Vol. 2.  
23  
24  
25 29. Bowers, K. J.; Chow, E.; Xu, H.; Dror, R. O.; Eastwood, M. P.; Gregersen, B. A.;  
26 Klepeis, J. L.; Kolossvary, I.; Moraes, M. A.; Sacerdoti, F. D.; Salmon, J. K.; Shan, Y.;  
27 Shaw, D. E. *Scalable Algorithms for Molecular Dynamics Simulations on Commodity*  
28 *Clusters* Proceedings of the ACM/IEEE Conference on Supercomputing (SC06), Tampa,  
29 Florida, **2006**, November 11-17.  
30  
31  
32  
33  
34 30. Desmond Molecular Dynamics System, D. E. Shaw Research, New York, NY, **2018**.  
35  
36  
37 31. GaussView, Version 5, Roy Dennington, Todd Keith, John Millam. Semichem Inc.,  
38 Shawnee Mission, KS, **2009**.  
39  
40  
41 32. Frisch, M. J.; Trucks, G. W.; Schlegel, H. B.; Scuseria, G. E.; Robb, M. A.; Cheeseman,  
42 J. R.; Scalmani, G.; Barone, V.; Petersson, G. A.; Nakatsuji, H.; Li, X.; Caricato, M.;  
43 Marenich, A.; Bloino, J.; Janesko, B. G.; Gomperts, R.; Mennucci, B.; Hratchian, H. P.;  
44 Ortiz, J. V.; Izmaylov, A. F.; Sonnenberg, J. L.; Williams-Young, D.; Ding, F.; Lipparini,  
45 F.; Egidi, F.; Goings, J.; Peng, B.; Petrone, A.; Henderson, T.; Ranasinghe, D.;  
46 Zakrzewski, V. G.; Gao, J.; Rega, N.; Zheng, G.; Liang, W.; Hada, M.; Ehara, M.;  
47 Toyota, K.; Fukuda, J.; Hasegawa, J.; Ishida, M.; Nakajima, T.; Honda, Y.; Kitao, O.;  
48 Nakai, H.; Vreven, T.; Throssell, K.; Montgomery, J. A.; Peralta, J. E.; Ogliaro, F.;  
49 Bearpark, M.; Heyd, J. J.; Brothers, E.; Kudin, K. N.; Staroverov, V. N.; Keith, T.;  
50  
51  
52  
53  
54  
55  
56  
57  
58  
59  
60

- 1  
2  
3 Kobayashi, R.; Normand, J.; Raghavachari, K.; Rendell, A.; Burant, J. C.; Iyengar, S. S.;  
4 Tomasi, J.; Cossi, M.; Millam, J. M.; Klene, M.; Adamo, C.; Cammi, R.; Ochterski, J.  
5 W.; Martin, R. L.; Morokuma, K.; Farkas, O.; Foresman, J. B.; Fox, D. J. Gaussian 09,  
6 Revision A.02; Gaussian, Inc.: Wallingford, CT, USA, **2009**.
- 7  
8  
9  
10  
11 33. Lakowicz, J. R. Principles of Fluorescence Spectroscopy. Springer Science & Business  
12 Media, **1999**.
- 13  
14  
15 34. Wang, Y. -Q.; Zhang, H. -M.; Zhang, G. -C.; Tao, W. -H.; Tang, S. -H. Interaction of the  
16 flavonoid hesperidin with bovine serum albumin: a fluorescence quenching study. *J.*  
17 *Lum.* **2007**, 126, 211–218.
- 18  
19  
20  
21 35. Soares, S.; Mateus, N.; Freitas, V. Interaction of Different Polyphenols with Bovine  
22 Serum Albumin (BSA) and Human Salivary  $\alpha$ -Amylase (HSA) by Fluorescence  
23 Quenching. *J. Agric. Food Chem.*, **2007**, 55, 6726–6735.
- 24  
25  
26  
27 36. Zhang, X.; Chytil, P.; Etrych, T.; Liu, W.; Rodrigues, L.; Winter, G.; Filippov, S. K;  
28 Papadakis, C. M. Binding of HSA to Macromolecular pHPMA Based Nanoparticles for  
29 Drug Delivery: An Investigation Using Fluorescence Methods. *Langmuir*. **2018**, A-I.
- 30  
31  
32  
33 37. Zhao, Y.; Yang, H.; Meng, K.; Yu, S. Probing the Ca<sup>2+</sup>/CaM-induced secondary  
34 structural and conformational changes in calcineurin. *Int. J. Biol. Macromol.* **2014** 4,  
35 453–457.
- 36  
37  
38  
39 38. Bello, M.; Correa-Basurto, J.; PLoS One. **2013**, 8, 1–13.
- 40  
41  
42 39. Niu, X.; Gao, X.; Wang, H.; Wang, X.; Wang, S. Insight into the dynamic interaction  
43 between different flavonoids and bovine serum albumin using molecular dynamics  
44 simulations and free energy calculations. *J. Mol. Model.* **2013**, 19, 1039–1047.
- 45  
46  
47 40. Wang, H.; Tang, Y.; Lei, M. Models for binding cooperativities of inhibitors with  
48 transthyretin. *Arch. Biochem. Biophys.* **2007**, 466, 85–97.
- 49  
50  
51  
52 41. Shahlaei, M.; Rahimi, B.; Ashra-Kooshk, M. R.; Sadrjavadi, K.; Khodarahmi, R. Probing  
53 of possible olanzapine binding site on human serum albumin: Combination of  
54 spectroscopic methods and molecular dynamics simulation. *J. Lumin.* **2015**, 158, 91–98.
- 55  
56  
57  
58  
59  
60

- 1  
2  
3 42. Zhang, L.; Sun, Y. Biomimetic Design of Platelet Adhesion Inhibitors to Block Integrin  
4  $\alpha 2\beta 1$ -Collagen Interactions: I. Construction of an Affinity Binding  
5 Model. *Langmuir*. **2014**, 30, 4725–4733.  
6  
7  
8  
9 43. Politzer, P.; Murray, J.S.; Peralta-Ingá, Z. Molecular surface electrostatic potentials in  
10 relation to noncovalent interactions in biological systems. *Int. J. Quantum. Chem.* **2001**,  
11 81, 676-684.  
12  
13  
14  
15 44. Roy, D.R.; Sarkar, U.; Chattaraj, P.K.; Mitra, A.; Padmanabhan, J.; Parthasarathi, R.;  
16 Subramanian, V.; Damme, S.V.; Bultinck, P. Analyzing toxicity through Electrophilicity.  
17 *P. Mol Divers.* **2006**, 10, 119–131.  
18  
19  
20  
21 45. Parr, R.G.; Szentpály, L.V.; Liu, S. Electrophilicity Index. *J. Am. Chem. Soc.* **1999**, 121,  
22 1922–1924.  
23  
24  
25 46. Parr, R.G.; Pearson, R.G. Absolute Hardness: Companion parameter to absolute electro  
26 negativity. *J. Am. Chem. Soc.* **1983**, 105, 7512–7516.  
27  
28  
29  
30 47. Geerlings, P.; Proft, F.D. Langencker, W. Conceptual density functional theory. *Chem.*  
31 *Rev.* **2003**, 103, 1793–1873.  
32  
33  
34 48. Roy, D.R.; Parthasarathi, R.; Maiti, B.; Subramanian, V.; Chattaraj, P.K. Electrophilicity  
35 as a possible descriptor for toxicity prediction. *Bioorg. Med. Chem.* **2005**, 13, 3405–3412  
36  
37  
38 49. Fukui, K. Role of Frontier orbitals in chemical reactions. *Science*. **1982**, 218, 747-754  
39  
40  
41 50. Xie-Mei Dong; Yan-Yue Lou; Kai-Li Zhou; Jie-Hua Shi. Exploration of association of  
42 telmisartan with calf thymus DNA using a series of spectroscopic methodologies and  
43 theoretical calculation. *J Mol Liq.* **2018**, 266, 1-9.  
44  
45  
46  
47 51. Jie-Hua Shi; Kai-Li Zhou; Yan-Yue Lou; Dong-Qi Pan. Multispectroscopic and molecular  
48 docking studies on the interaction of darunavir, a HIV protease inhibitor with calf thymus  
49 DNA. *Spectrochim Acta A Mol Biomol Spectrosc.* **2018**, 193, 14-22.  
50  
51  
52  
53  
54  
55  
56  
57  
58  
59  
60

- 1  
2  
3  
4  
5  
6  
7  
8  
9  
10  
11  
12  
13  
14  
15  
16  
17  
18  
19  
20  
21  
22  
23  
24  
25  
26  
27  
28  
29  
30  
31  
32  
33  
34  
35  
36  
37  
38  
39  
40  
41  
42  
43  
44  
45  
46  
47  
48  
49  
50  
51  
52  
53  
54  
55  
56  
57  
58  
59  
60
52. Jie-Hua Shi; Yan-Yue Lou; Kai-Li Zhou; Dong-Qi Pan. Elucidation of Intermolecular Interaction of Bovine Serum Albumin with Fenhexamid: A Biophysical Prospect. *J Photochem Photobiol B*. **2018**, 180, 125-133.
53. QiWang; Chuan-ren Huang; Min Jiang; Ying-yao Zhu; JingWang; Jun Chen; Jie-hua Shi. Binding interaction of atorvastatin with bovine serum albumin: Spectroscopic methods and molecular docking. *Spectrochim Acta A Mol Biomol Spectrosc*. **2016**, 156, 155-163.
54. Jayant I. Gowda; Sharanappa T. Nandibewoor. Binding and conformational changes of human serum albumin upon interaction with 4-aminoantipyrine studied by spectroscopic methods and cyclic voltammetry. *Spectrochim Acta A Mol Biomol Spectrosc*. **2014**, 124, 397-403.
55. Keerti M. Naik; Sharanappa T. Nandibewoor. Spectral characterization of the binding and conformational changes of bovine serum albumin upon interaction with an anti-fungal drug, methylparaben. *Spectrochim Acta A Mol Biomol Spectrosc*. **2013**, 105, 418-423.
56. Keerti M Naik; Deepa B Kolli; Sharanappa T Nandibewoor. Elucidation of binding mechanism of hydroxyurea on serum albumins by different spectroscopic studies. *SpringerPlus*. **2014**, 3(360), 1-13.
57. Praveen N. Naik; Shivamurti A. Chimatadar; Sharanappa T. Nandibewoor. Pharmacokinetic Study on the Mechanism of Interaction of Sulfacetamide Sodium with Bovine Serum Albumin: *A Spectroscopic Method. Biopharm. Drug Dispos*. **2010**, 31, 120 – 128.
58. Prashant A. Magdum; Naveen M. Gokavi; Sharanappa T. Nandibewoor. Study on the interaction between anti-tuberculosis drug ethambutol and bovine serum albumin: multispectroscopic and cyclic voltammetric approaches. *Luminescence*. **2017**, 32(2), 206-216
59. Arunkumar T. Buddanavar; Sharanappa T. Nandibewoor. Multi-spectroscopic characterization of bovine serum albumin upon interaction with atomoxetine. *J. pharm. anal*. **2017**, 7, 148-155.

## Graphical TOC Entry



Interaction plot of NANA after MD simulation

